

***Mechanical and Energy Engineering***

**Geomechanical study to predict the onset of sand production formation**

**Tahseen Khudair Yosif**  
University of Baghdad  
College of Engineering  
Iraq-Baghdad  
[mac.tah.eng80@gmail.com](mailto:mac.tah.eng80@gmail.com)

**Dr. Jalal A. Al-Sudani**  
University of Baghdad  
College of Engineering  
Iraq-Baghdad  
[jalsud@uobaghdad.edu.iq](mailto:jalsud@uobaghdad.edu.iq)

**ABSTRACT**

One of the costliest problems facing the production of hydrocarbons in unconsolidated sandstone reservoirs is the production of sand once hydrocarbon production starts. The sanding start prediction model is very important to decide on sand control in the future, including whether or when sand control should be used. This research developed an easy-to-use Computer program to determine the beginning of sanding sites in the driven area. The model is based on estimating the critical pressure drop that occurs when sand is onset to produced. The outcomes have been drawn as a function of the free sand production with the critical flow rates for reservoir pressure decline. The results show that the pressure drawdown required to produce a free sand oil flow rate reduces with the skin factor increasing. Moreover, free sand oil production cannot be prevented at well-flowing pressure of 500 psi.

**Keywords:** Logging data, sand prediction, rock mechanics parameter, interface drawdown pressure.

**دراسة جيوميكانيكية للتنبؤ ببدء إنتاج الرمل**

د. جلال عبد الواحد  
أستاذ مساعد  
كلية الهندسة – جامعة بغداد

تحسين خضير يوسف  
باحث  
جامعة بغداد/ كلية الهندسة

**الخلاصة**

من أكثر المشاكل تكلفة التي تواجه إنتاج الهيدروكربونات في الخزانات غير المتصلة من الحجر الرملي إنتاج الرمل بمجرد بدء إنتاج الهيدروكربونات. ونموذج التنبؤ ببدء الصنفرة مهم جدًا، من أجل اتخاذ قرار التحكم في الرمال في المستقبل، عندها يجب

\*Corresponding author

Peer review under the responsibility of University of Baghdad.

<https://doi.org/10.31026/j.eng.2022.02.01>

2520-3339 © 2022 University of Baghdad. Production and hosting by Journal of Engineering.

This is an open access article under the CC BY4 license <http://creativecommons.org/licenses/by/4.0/>.

Article received: 30 /6 /2021

Article accepted: 31/8/2021

Article published:1/2/2022



استخدام التحكم أم لا، أو عند استخدام التحكم بالرمل. قمنا بتطوير برنامج كمبيوتر سهل الاستخدام لتحديد بداية مواقع الصنفرة في المنطقة المدفوعة، ويستند هذا النموذج إلى تقدير انخفاض الضغط الحرج الذي يحدث عند بدء إنتاج الرمال. تم رسم النتائج كدالة لإنتاج الرمال الحرة مع معدلات التدفق الحرجة المسموح بها كدالة لانخفاض ضغط المكنن. أظهرت النتائج أن انخفاض الضغط المطلوب لإنتاج معدل تدفق حر للنفت مع الرمل يقل مع زيادة عامل التضرر. علاوة على ذلك، وجد أنه عند ضغط تدفق البئر البالغ 500 رطل / بوصة مربعة. لا يمكن منع إنتاج الرمل مع النفط. الكلمات الرئيسية: ادخال البيانات، التنبؤ ببدء إنتاج الرمل، معامل الصخور الميكانيكي، ضغط تدفق البئر

## INTRODUCTION

The problem of sand production is one of the old problems in the oil industry. Authors have been interested in this problem since the beginning of knowing the oil industry and trying to find solutions to it. This article used an analytical model to predict sand production, which has good potential for field application. It must be understood that in order to obtain a reliable sand production forecast, the production official must study the field data well and accurately. It is necessary to have a correct and accurate understanding of geomechanics to provide data for future reservoir pressure and subsidence in order to have a clear idea of sand production. Also, this work needs to determine the pressures at the walls of the holes or the well, if these induced pressures exceed the strength of the formation at the site, the formation will fail, and sand can be produced with reservoir fluids. Also, sanding prediction needs to know the mechanisms by which the collapse of the rocks of the producing layer will occur. Therefore, it is important to identify the mechanism that caused the formation instability problem. Sand production occurs when the pressure on the formation exceeds the strength of the formation and leads to the collapse of the rocks. Rock failure also occurs due to tectonic activities, excessive stress, pore pressure, and pressure during drilling. Depending on the available data set, there is a need to determine and estimate some geomechanical parameters. The properties can be estimated using empirical correlations with measured acoustic velocities. In this paper, the acoustic log, which measures the time of transmitting sound waves through the different layers, determined sand production well. Input parameters required for the application use the appropriate parameters where these parameters, whether physical or geomechanical, such as elasticity and strength of rocks as well as pore pressure and local pressures.

In this work, the geomechanical properties were determined using the well logs for some wells in Nahr Umr Formation (N-R) - Amara oil reservoir, which is considered as one of the important oil reservoirs in Iraq. The one problem in this reservoir is producing sand in large quantities, which sometimes leads to the well's closure and thus leads to a shortage or absence of production. The geomechanical properties of the reservoir rocks have been determined; this will be very useful in the model used.

## Factors affecting sand production

Many factors affect the ability of the layer to produce sand (Zhou et al., 2016). The solid particles that are produced from the reservoir rock through the hydrocarbon compounds produced are in the form of granules. As it is known that the production of sand from the layers produced during the production of hydrocarbon compounds has many risks, and to reduce these risks, it must be produced at pressure rates less than the expected critical pressure.



- **Degree of association:** association is a function of the mechanical parameter, the "compressive strength," Which shows how strongly bound sand grains are bound to each other.
- **Production rate:** The production of hydrocarbons from the reservoir causes two forces, a differential pressure force and a frictional force. These two forces form a force that can exceed the formation's compressive strength. It is an indication of a critical flow rate of the producing layer. It means the flow rate at which sand begins to produce with the produced fluids.
- **Drawdown:** Continuous gradient can affect sand transmission. Any change in flow rate or production cessation may lead to the collapse of the formation sand, resulting in sand production until a new arc formation is formed.
- **Reduction of Pore Pressure:** Reducing reservoir pressure increases pressure on the formation sand itself. The pressure of the reservoir rocks due to the low pore pressure can lead to subsidence of the surface.
- **The viscosity of Reservoir Fluids:** High viscosity reservoir fluids cause greater frictional drag force on sand grains than low viscosity reservoir fluid. The effect of viscous drag on sand production in high viscosity oil reservoirs is evident even at low flow velocities.
- **Increased water production:** Sand production has been observed to increase or start when water begins to produce or with increased water interruption.

The input data for this study consists of the well log records (acoustic, density, gamma rays, resistance, neutron porosity records). The study was conducted for a group of wells bearing the code name (X-5),(X-6),(X-10) for ownership reasons. The mechanical properties of rocks were classified into elastic and inelastic properties (Abijah and Tse, 2016). Mechanical rock properties were determined using density and sonic compressional ( $\Delta T_c$ ) and shear ( $\Delta T_s$ ) transit times. The elastic properties included Poisson ratio ( $\nu$ ), shear modulus (G), strength which includes uniaxial compressive strength, Biot's coefficient, tensile and cohesive strengths, and frictional angle, young's modulus ( $E$ ), bulk modulus (Kb) and bulk compressibility(CB) and grain compressibility (CR). This is properties Determination from P- and S- wave velocity. Since the shear wave is not available in the data, so the shear wave was estimated and used in the solution. This was achieved using the available relationships (Abijah and Tse, 2016).

$$V_p = \frac{304878}{\Delta T_c} \tag{1}$$

The following equation estimates the velocity of the shear wave through sandstone (John et al., 2020).

$$V_s = (0.804 * V_p) - 0.856 \tag{2}$$

Where  $V_s$  and  $V_p$  are shear wave and compressional wave velocities with unit Km/s



**The Control Layer Method**

Models for sand production must be created using field data, particularly strength formation data. Where basic information is not available, to estimate the strength of the formation required to be studied, the production engineer must rely on the parameters obtained from field records and use the appropriate equations. Therefore, this particular layer is called a control layer with minimal regression. A higher flow rate may cause another layer of sanding to occur. The general critical rate for the entire production period is estimated by determining the critical regression corresponding to the weakest region of the producing layer with respect to sand production. This work focused on the weakest area in the layer producing hydrocarbons during the production period, and this area is known as the area from which sand will be produced when the pressure is reduced. The critical pressure is used as a function of the separating pressure in the weak areas, and this pressure was reached through the mechanical and physical properties of the rocks using audio recordings, density, neutron, and other information (Awal and Osman, 1999).

The total critical flow is estimated by adopting the following stages:

- 1- Dividing the produced layer into multiple layers, possibly ten or more layers (the division was done for each unit length). Then enter the available data in a calculator program, which uses Excel, and the data parameters are;

Pe, Pp, Vsh, V, E, Dtc, h, S, B, μ, α,

- 2- After estimating the critical pressure of the weakest layer, the critical production rate is obtained for each area in the productive layer, and this is done using the Darcy equation, assuming that the shape of the well is vertical and circular. Darcy flow equation for the radial flow (Awal and Osman, 1999) is presented as follows:

$$q = \frac{7.08 \times 10^{-3} k_* h (P_R - P_{wf})}{B \mu \left[ \ln \frac{r_e}{r_w} - 0.75 + S_t \right]} \tag{3}$$

Obtain  $q_{crit}^{(1)} \cdot q_{crit}^{(2)} \cdot q_{crit}^{(3)} \cdot \dots \cdot q_{crit}^{(n)}$

Where,

i=1, 2, 3, ..., n

- 3- Calculate  $\Delta P_{dd}^{(i)}$  using Darcy’s equation for radial flow. Then select the minimum  $\Delta P_{dd}$

$$\Delta P_{dd}^{(i)} = \frac{B_o \mu_o q_{crit} \ln \left( \frac{r_e}{r_w} \right)}{0.00708 k^{(i)} h^{(i)}} \tag{4}$$

$$\Delta P_{dd}^* = \min \left( P_{wf}^{(1)} \cdot P_{wf}^{(2)} \cdot P_{wf}^{(3)} \cdot \dots \cdot P_{wf}^{(n)} \right) \tag{5}$$

For i=1, 2, 3, ..., n



Where

$\Delta P_{dd}^*$  Minimum drawdown

4- Calculate the total critical production rate of the entire stratum for each region, and then take the corresponding minimum downhole pressure, using the permeability and total thickness of the pay zone.

$$Q_{crit}^* = \frac{0.00708 \cdot h \cdot \Delta P_{dd}^*}{B_o \cdot \mu_o \cdot \ln\left(\frac{re}{rw}\right)} \tag{6}$$

Where

$Q_{crit}^*$  is the critical flow rate of the well,  $\Delta P_{dd}^*$  is the minimum drawdown,  $B_o$  is the oil formation volume factor,  $\mu_o$  is the oil viscosity,  $re$  is the radius of drainage,  $rw$  is the radius of wellbore,  $h$  is the total thickness of the pay zone.

**Estimating the input parameters**

Here are the parameters required to apply this method, and the calculation is done using field data. These parameters represent the mechanical and physical properties of the rocks of the producing layer. The objective of the field application of sand production models is to determine the ability of the layer to produce sand, and this is done using input data, especially formation strength data. Therefore, the field engineer has to rely on the correlation of parameters obtained from the well logs to assess the strength of the formation.

**Poisson Ratio (v)**

Poisson ratio (v) was computed from acoustic measurements, including the slowness of the compressional wave ( $\Delta T_c$ ) and shear wave ( $\Delta T_s$ ) ratio using the relationships (**Semester and Signature, 2011**).

$$v_{dyn} = \frac{\frac{1}{2} \left(\frac{\Delta t_s}{\Delta t_c}\right)^2 - 1}{\left(\frac{\Delta t_s}{\Delta t_c}\right)^2 - 1} \tag{7}$$

**Shear Modulus (G)**

The shear modulus (G) was estimated by using the following relationships (**Sulaimon and Teng, 2020**):

$$G = \frac{\rho}{\Delta t_s^2} \times 1.34 \times 10^{10} \tag{8}$$



**Bulk Modulus (Kb)**

The bulk modulus (Kb) was estimated from the sonic and density log using the following relationships (Tabrizy and Mirzaahmadian, 2012):

$$K_B = \rho_b \left( \frac{1}{\Delta t_c^2} - \frac{4}{3\Delta t_s^2} \right) * 1.34 * 10^{10} \tag{9}$$

**Young’s Modulus (E)**

The Young’s modulus was determined from the relationship (Udebhulu and Ogbe, 2015):

$$E = 2 * G * (1 + \nu) \tag{10}$$

**Rock modulus**

The rock modulus ( $K_R$ ) was estimated from the sonic and density logs using the relationships (Udebhulu and Ogbe, 2015):

$$K_R = \rho_{gr} \left( \frac{1}{\Delta t_{mc}^2} - \frac{4}{3\Delta t_{ms}^2} \right) * 1.34 * 10^{10} \tag{11}$$

**Bulk Compressibility**

Bulk compressibility (Cb) with porosity and rock compressibility (Cr) zero porosity was determined by the relationship in equation (Udebhulu and Ogbe, 2015):

$$C_B = \frac{1}{K_B} \tag{12}$$

$$C_R = \frac{1}{K_R} \tag{13}$$

**Determination of overburden pressure**

The pressure of overloading at a certain point in the layer results from the weight of the formation above it (Ashoori et al., 2014).

$$\sigma_v = g \int_0^z \rho(z) dz \approx \bar{\rho} g z \tag{14}$$



Where

$Z$  is the depth under the surface, and  $g$  is the ground acceleration.

**The compressional and shear sonic wave**

The movement of a compressed wave is parallel to the propagation line of the wave passing through the formation. While the shear wave movement in a perpendicular direction to the line of propagation of the traveling wave. The compressed wave velocity is measured directly from the sonic log records, while the shear wave velocity is estimated using available empirical equations. The sound wave is one of the main factors in determining the mechanical properties of the layers. There are three known experimental methods (Ismail et al., 2020):

a- Castagna equation (Ismail et al., 2020):

$$V_s = -0.05509V_p^2 + 1.0168V_p - 1.0305 \tag{15}$$

b- Brocher equation (Ismail et al., 2020):

$$V_s = 0.7858 - 1.2344V_p + 0.7949V_p^2 - 0.1238V_p^3 + 0.006V_p^4 \tag{16}$$

c- Carroll equation (Ismail et al., 2020):

$$V_s = 1.09913326 \times V_p^{0.9238115336} \tag{17}$$

**Sand Production Prediction Model: Input Parameters**

The main parameters required to evaluate sand production prediction are rock strength data (UCS-uniaxial compressive strength), subsurface stresses (vertical, minimum, and maximum horizontal stress value and azimuth maximum horizontal stress), reservoir pressures, and the effect of pressure depletion (Subbiah et al., 2020).

**Unconfined compressive strength (UCS)**

It is an indicator scale for the strength of the formation. It also indicates the maximum compressive stress, which the layer can withstand when unconfined. Many relationships relate the strength of formation rocks to parameters that can be measured in the geophysical records. These parameters such as the elastic coefficients, density, Compressional, and shear wave velocity. For sedimentary rocks, the UCS can be calculated as follows (Ismail et al., 2020):

$$UCS = 0.008EV_{sh} + 0.0045E(1 - V_{sh}) \tag{18}$$

Where,



$V_{sh}$  is the volume of shale, and E is the young's modulus.

**Stress analysis**

The stresses inside and around the well can be estimated where the borehole or holes are often considered to be a thick, hollow cylinder. Thus, the distribution of stresses around the borehole can be obtained. There are many factors affecting stresses, including tectonic forces and the weight of the upper layers. The following are the three-axis stress equations used (Ismail et al., 2020):

$$\sigma_x = mP_o + \alpha P_p(1 - m) \tag{19}$$

$$\sigma_y = mP_o + \alpha P_p(1 - m) \tag{20}$$

$$m = \frac{V}{1 - V} \tag{21}$$

$$\sigma_z = P_o \tag{22}$$

Where:

V is the Poisson's ratio, Po is the overburden pressure, Pp is the pore pressure, and  $\sigma_x, \sigma_y, \sigma_z$  are the principal stresses

**Critical wellbore pressure**

Sand production in wells and holes in sandstone reservoirs is critical. To estimate the risks of sand production for a field during its production period, a calculation should be made for critical wellbore pressure. Critical well pressure is the minimum pressure of a well at which this amount of pressure can continue to produce hydrocarbon without producing sand together.

(Ismail et al., 2020), it can be presented as follows:

$$\tau_i = \frac{0.025UCS}{10^6 C_B} \tag{23}$$

The critical wellbore pressure can be determined as follows:

$$P_c = \frac{1.5\sigma_x - 0.5\sigma_y - 0.5\alpha P_p \left(\frac{1 - 2\nu}{1 - \nu}\right) - 1.732\tau_i}{1 - 0.5\alpha \left(\frac{1 - 2\nu}{1 - \nu}\right)} \tag{24}$$

Where





$V$  is the Poisson's ratio,  $P_o$  is the overburden pressure,  $P_p$  is the pore pressure,  $\sigma_x$ ,  $\sigma_y$ ,  $\sigma_z$  are the principal stresses,  $t_i$  is the initial shear strength of rock and  $P_c$  is the Critical flowing wellbore pressure.

### Availability of registration data

- 1- Depth.
- 2- Density.
- 3- Compressional wave.
- 4- Gamma-ray.
- 5- Porosity.

### Sonic Log

A sound record is an important tool, which can be used in calculations to predict sand production from wells. In contrast, the sonic log records the time required to transmit sound waves through the different layers. There is a relationship between porosity and the transmission time of sound waves. Where short times indicate, for sandy layers (e.g., 50 microseconds) indicates low porosity and that the rocks are solid and dense. Whereas longer transition periods (e.g., 95 microseconds or more) indicate softer rocks have higher porosity. So sand production must be linked to the audio recording readings (John et al., 2020).

### Volume of shale

Many researchers studied the relationship between the clay content and the sound waves transmission time, as they found a decrease in the speed of sound waves with an increase in the clay content. This is due to the increased compaction of the clay layers. They also noticed that the clay affects the petrophysical properties by reducing the pore volume and the pressure of the layer containing the clay. The volume of clay can be estimated using gamma rays and the Larionov equation (John et al., 2020).

$$V_{sh} = 0.33 \left( 2^{(2^{I_{gr}})} - 1 \right) \quad (25)$$

### Neutron log

The neutron recording measures the hydrogen concentration in the different layers. The recording can be interpreted as a porosity index. When a high concentration of hydrogen is measured in the neighboring rocks, and because the liquids are in large quantities, it can be explained that the porosity is high. While a small concentration of hydrogen was recorded because of the few liquids present, this indicates that the porosity of the area is low (Onalo et al., 2020).



**Area of the Study**

The study relied in particular on well X.10, as it is considered one of the modern wells, and production is underway. The depth of the studied rocks in the ground varies according to the **N-R** layer and the formation whose stratigraphic series consists of loose sandstones and intertwined rocky rocks such as clay. The resilience and strength properties of the rocks obtained from the empirical relationships are summarized in **Tables 1 and 2.**

**Table 1.** Geophysical properties

vsh	Dts -msec/ft	GR	DT- msec/ft	RHOB- gm/cc	Depth- ft	Region
0.02	87.55	17.63	56.28	2.59	11696	Region.1
0.27	103.25	47.32	64.22	2.14	11807.6	Region.2

**Table 2.** Mechanical properties.

Cr(psi)	Kr(psi)	Cb (psi <sup>-1</sup> )	Kb(psi)	E(psi)	G(psi)	Region
2.00678E-07	4983107.4	2.0279E-07	4931052	1042049	4539106	Region.1
2.42404E-07	4125340.5	2.9577E-07	3381008	6400593	2701851	Region.2

**Well-X.10**

The reservoir data are presented in table 3. Rock mechanical properties such as elastic dynamics and other data relevant to sand production were estimated as described below based on the well log data. This well was studied at a depth ranging between 11518-12100 feet, and the results were as shown in table-3. **Fig.1** shows the well's mechanical properties, including Poisson's ratio, Biot's constant, Flowing bottom hole pressure, principal stresses at direction x, Unconfined compressive strength (UCS), and critical flow rate.

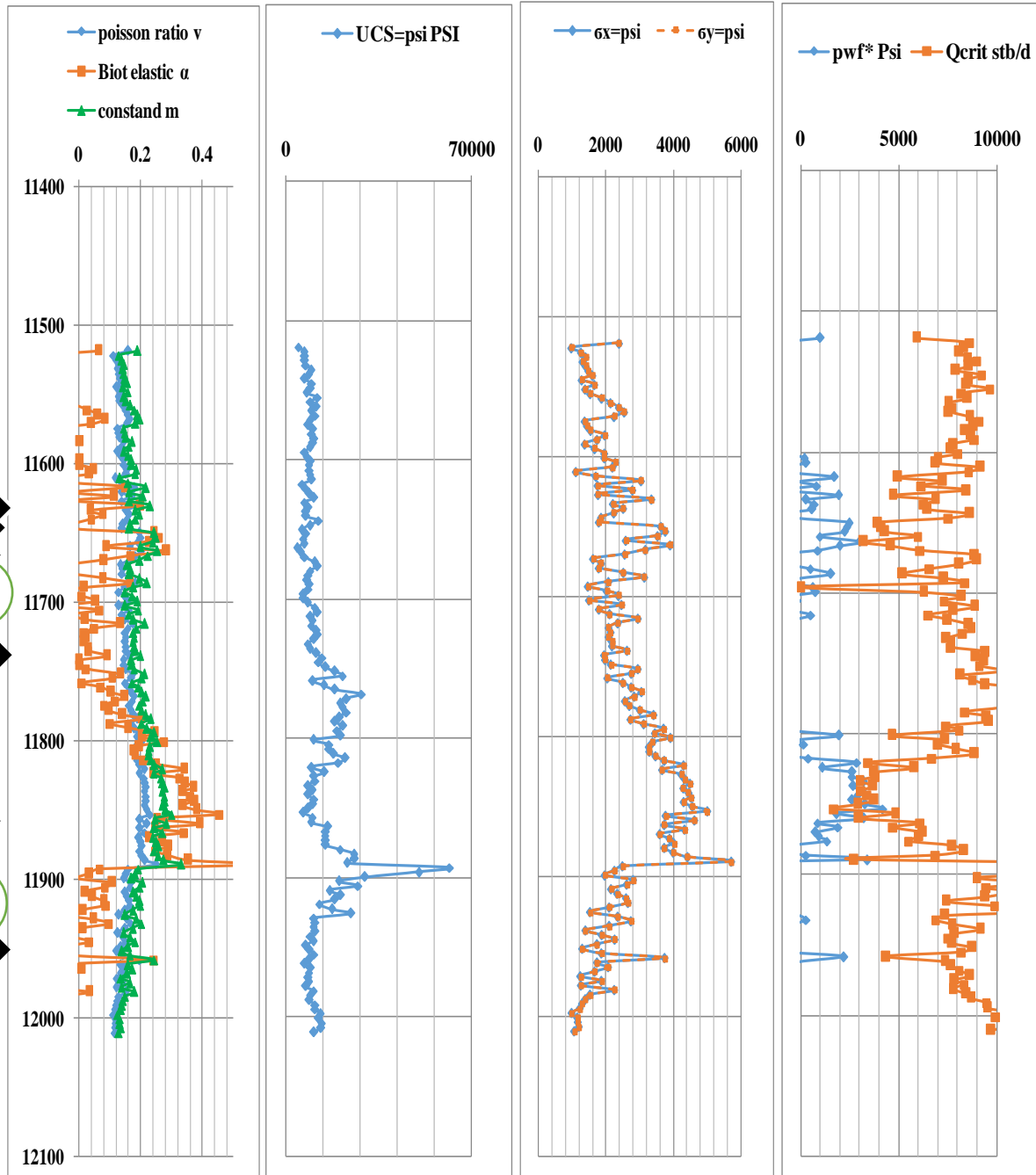


Table 3. The reservoir data.

Dts	vsh	GR	DT	RHOB	Depth
msec/ft		API	( $\mu$ sec/ft	Gm/cc	ft
92.19955	0.006903	14.5243	58.635	2.5117	11518.9
77.56742	0.007806	14.7099	51.2358	2.7005	11522.2
80.1746	0.014187	15.9827	52.5542	2.6957	11525.5
81.48451	0.014835	16.1084	53.2166	2.7008	11528.7
80.59739	0.020373	17.1593	52.768	2.7095	11532
81.50923	0.040874	20.7351	53.2291	2.7233	11535.3
82.27374	0.033898	19.5674	53.6157	2.716	11538.6
83.43495	0.019892	17.0696	54.2029	2.715	11541.9
80.33557	0.040123	20.6116	52.6356	2.7298	11545.1
83.99518	0.046151	21.5895	54.4862	2.7135	11548.4
81.29348	0.02327	17.6929	53.12	2.714	11551.7
82.75112	0.073098	25.6322	53.8571	2.697	11555
86.19597	0.050476	22.2728	55.5991	2.6826	11558.3
89.12291	0.085749	27.3786	57.0792	2.6868	11561.5
92.054	0.068747	25.0113	58.5614	2.6752	11564.8
93.96865	0.095208	28.6323	59.5296	2.6706	11568.1
90.27799	0.058557	23.5119	57.6633	2.6579	11571.4
81.13291	0.029672	18.8367	53.0388	2.6876	11574.7
81.79953	0.050694	22.3069	53.3759	2.6714	11577.9
82.82587	0.048551	21.9705	53.8949	2.6766	11581.2
87.1616	0.070321	25.2373	56.0874	2.6303	11584.5
84.75317	0.059934	23.7185	54.8695	2.654	11587.8
81.12935	0.037993	20.2583	53.037	2.6842	11591.1



84.01258	0.020759	17.2309	54.495	2.6937	11594.3
87.00478	0.034587	19.6847	56.0081	2.6718	11597.6
87.0204	0.053046	22.672	56.016	2.6561	11600.9



**Figure 1.** Poisson’s ratio, properties of rocks, Unconfined compressive strength (UCS),  $Q_{crit}^*$  the critical flow rate, pwf Critical flowing wellbore pressure, psi versus depth.



However, table.4 shows seven levels of **N-R** sand formation, as indicated in **Fig. 1**. It presents low flowing well pressure in ascending sequence. These levels should be prevented in any perforation process to avoid sand production

**Table 4.** Minimum PWF where sanding occurs

No	Minimum-pwf-psi	Depth-ft
1	132.6	11696.1
2	177.8	11604.2
3	245.8	11886.3
4	254.7	11607.5
5	271.1	11633.7
6	279.9	11932.3
7	395.7	11817.4

**RESULTS and DISCUSSION**

This method was applied in the field on well No. 10, where the results are obtained. Among the important observations in this well, two weak areas were found in the producing layer with the same specifications but at different depths. The first region is at a depth of 11696 feet, and the second region is at a depth of 11807.6 feet.

**Figures 2, 3, 4, and 5** show the outcomes of the computer program made to estimate the critical flow rate for the sanding control layer for skin factors of zero, 5, 10, and 20, respectively. These figures show the free sand production with the critical flow rates, which are considered a function of reservoir pressure decline.

It can be noticed that the pressure drawdown required to produce a free sand oil flow rate reduces with the increase of skin factor.

However, unlike carbonate formations, the stimulation of sandstone formation cannot improve the skin less than its original permeability (Skin=0); therefore, the generated plots are restricted to skins greater than zero.

These figures show that at well flowing pressure of about 500 psi; the free sand oil production cannot be prevented; however, this pressure is less than the bubble point pressure, which is



conventionally not allowed to be reached by the oil companies. Thus, the limiting factor in this well will be the flow rate.

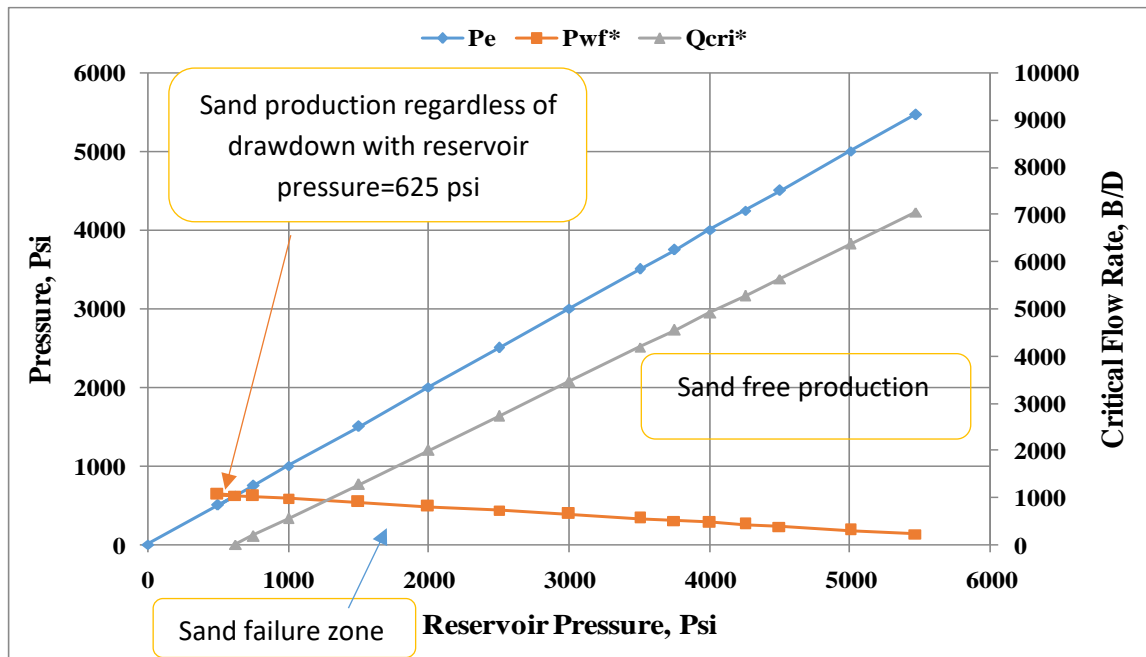


Figure 2. The relationship between reservoir pressure and downhole pressure for well X.10- in the case skin of zero.

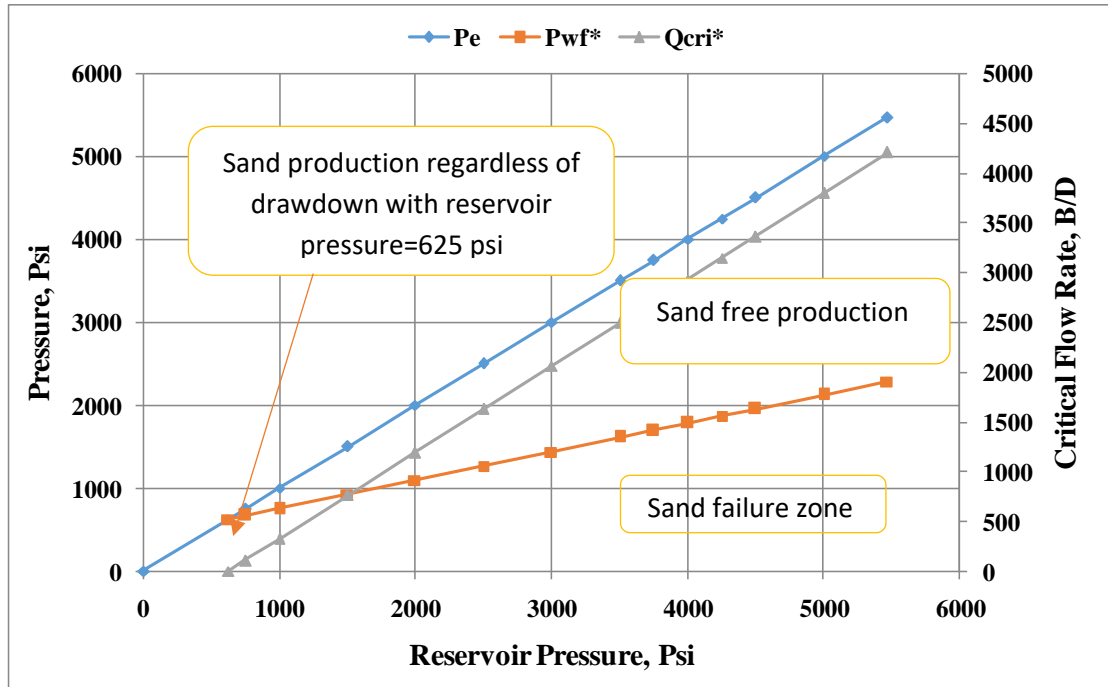


Figure 3. The relationship between reservoir pressure and downhole pressure for well X.10- in the case skin of 5.

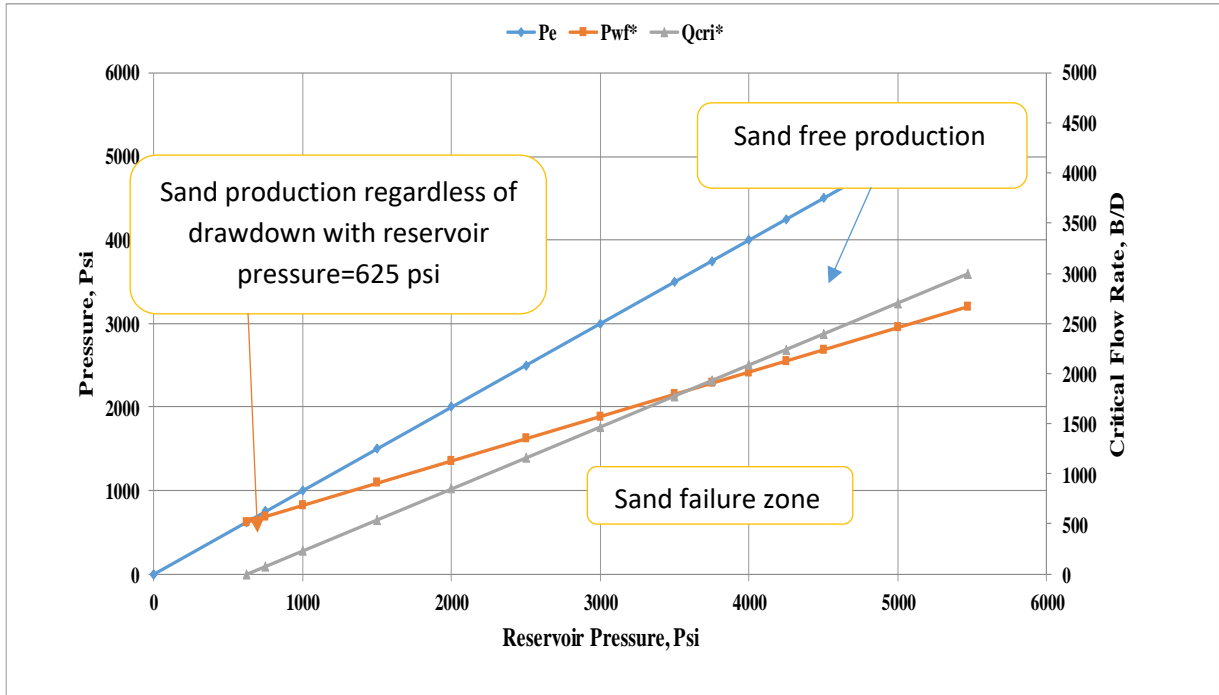


Figure 4. The relationship between reservoir pressure and downhole Pressure for well X-10- in the case skin of 10.

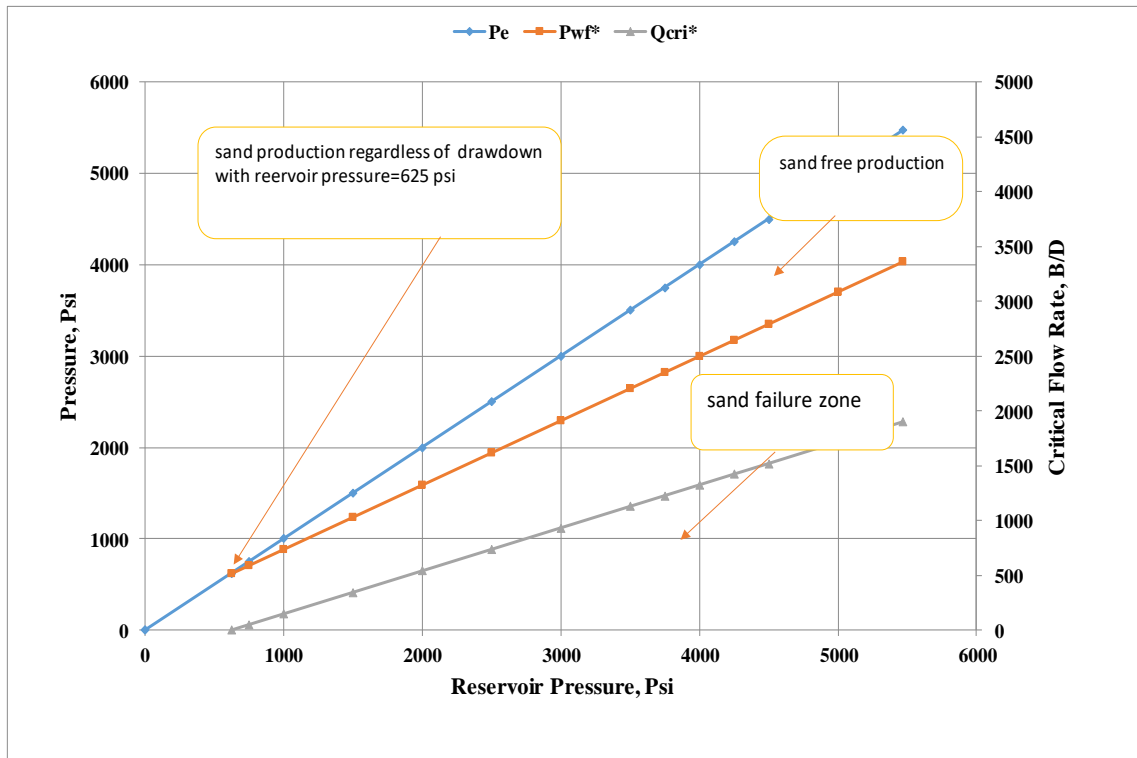


Figure 5. The relationship between reservoir pressure and downhole pressure for well X -10- in the case Skin of 20.



## CONCLUSIONS

1-The production engineer can perform sand forecast analysis in a specific area that needs a large amount of field data to be evaluated. The engineer can benefit from accessible calculator programs that facilitate the task.

2- The computational method, in the present research, uses critical flow rates for the produced layer based on the splitting of individual multilayers. It was observed that the expected critical flow rate is in good agreement with the observed data. However, the forecast is based on accurate field data for each region in the production period.

3- It is very important to determine the conditions under which sanding occurs to decide to control sand production. For this purpose, a new computing-based model has been developed to identify the weakest region within the productive layer. A field data set for three producing wells was used to build and test the model. The statistical and graphical results showed that the proposed model has a high classification power in determining the sanding conditions. Such results will facilitate decision-making strategies regarding sand control in the future.

## Nomenclature

B	oil formation volume factor
C <sub>b</sub>	Bulk Compressibility, psi <sup>-1</sup>
D <sub>tc</sub>	sonic compressional transit times
D <sub>ts</sub>	sonic shear transit times
E	Young Modulus, psi
G	Shear Modulus, psi
h	formation thickness, ft
k	formation permeability, md
P <sub>p</sub>	pore pressure, psi
P <sub>c</sub>	critical flowing wellbore pressure, psi
P <sub>b</sub>	bulk density of rock
P <sub>e</sub>	reservoir pressure
P <sub>o</sub>	overburden pressure
r <sub>e</sub>	radius of reservoir
r <sub>w</sub>	radius of wellbore
S	skin factors
t <sub>i</sub>	initial shear strength of rock
UCS	unconfined compressive strength
V	Poisson's ratio
V <sub>sh</sub>	volume of shale
V <sub>s</sub>	shear wave velocities
V <sub>p</sub>	compressional wave velocities
μ	fluid viscosity
α	Biot's constant
σ <sub>x</sub> , σ <sub>y</sub> , σ <sub>z</sub>	principal stresses along with the Cartesian coordinates





## REFERENCES:

- Abijah, F. A., and Tse, A. C., 2016. *Geomechanical Evaluation of an onshore oil field in the Niger Delta, Nigeria*. IOSR Journal of Applied Geology and Geophysics, p 4(1), 99–111. <https://doi.org/10.9790/0990-041199111>.
- Ashoori, S., Abdideh, M., Hayavi, M. T., and Branch, O., 2014. *Prediction of Critical Flow Rate for Preventing Sand Production Using the Mogi-Coulomb Failure Criterion*. Science International, p 26(5), 2029–2032.
- Awal, M. R., and Osman, E. S. A., 1999. *SandPro - a new application program for predicting onset of sand production*. *Proceedings of the Middle East Oil Show*, p 141–154.
- Ismail, N. I., Naz, M. Y., Shukrullah, S., and Sulaiman, S. A., 2020. *Mechanical earth modeling and sand onset production prediction for Well X in Malay Basin*. *Journal of Petroleum Exploration and Production Technology*, p 10(7), 2753–2758. <https://doi.org/10.1007/s13202-020-00932-2>.
- John, R. O., Temitope, O. F., Yunusa, O. C., Anthony, A. A., Efeoghene, E., Faith, E. I., and Amaechi, G. C., 2020. *Comparative Characterization of Petrophysical and Mechanical Properties of Siliciclastic Reservoir Rocks within a compressional structure of the Teapot Dome Oilfield, Wyoming, USA*. *Annals of Science and Technology*, p 5(2), 1–12. <https://doi.org/10.2478/ast-2020-0009>.
- Onalo, D., Adedigba, S., Oloruntobi, O., Khan, F., James, L. A., and Butt, S., 2020. *Data-driven model for shear wave transit time prediction for formation evaluation*. *Journal of Petroleum Exploration and Production Technology*, p 10(4), 1429–1447. <https://doi.org/10.1007/s13202-020-00843-2>.
- Semester, S., and Signature, A., 2011. *Analysis of borehole failure related to bedding plane*.
- Sulaimon, A. A., Teng, L. L., 2020. *Modified approach for identifying weak zones for effective sand management*. *Journal of Petroleum Exploration and Production Technology*, p 10(2), 537–555. <https://doi.org/10.1007/s13202-019-00784-5>.
- Subbiah, S. K., Samsuri, A., Hussein, A. M., Jaafar, M. Z., Chen, Y. R., and Kumar, R. R., 2020. *Root cause of sand production and methodologies for prediction*. *Petroleum*". <https://doi.org/10.1016/j.petlm.2020.09.007>.
- Tabrizy, V. A., and Mirzaahmadian, Y., 2012. *Investigation of Sand Production Onset : A New Approach Based on Petrophysical Logs*. SPE 150529 p 1, 1–18.
- Udebhulu, D. O., and Ogbe, D. O., 2015. *Mechanistic models for predicting sand production: A case study of Niger delta wells*. Society of Petroleum Engineers - SPE Nigeria Annual International Conference and Exhibition, NAICE 2015. <https://doi.org/10.2118/178279-ms>.
- Zhou, S. and F. Sun, 2016. *Sand Carrying in Wellbore and Surface Treatment of Produced Sands, Sand Prod. Manag. Unconsolidated Sandstone Reserve*, pp. 108–142, 2016, doi: 10.1002/9781118961865.ch5.